

Nanoparticulate Inhibitors of the Flavivirus Proteases from Zika, West Nile and Dengue Virus Are Cell-Permeable Antivirals

Barbara Schroeder,¹ Peter Demirel,¹ Christina Fischer,¹ Enaam Masri,¹ Stephanie Kallis,^{2,3} Lisa Redl,¹ Thomas Rudolf,¹ Silke Bergemann,¹ Christoph Arkona,¹ Christoph Nitsche,⁴ Ralf Bartenschlager,^{2,3} Jörg Rademann*¹

Please insert ORCID IDs here: Jörg Rademann: 0000-0001-6678-3165, Christoph Nitsche: 0000-0002-3704-2699, Ralf Bartenschlager: 0000-0001-5601-9307

¹ Pharmaceutical and Medicinal Chemistry, Institute of Pharmacy, Freie Universität Berlin, Königin-Luise-Straße 2+4, 14195 Berlin, Germany

² Department for Infectious Diseases, Molecular Virology, Heidelberg University, Im Neuenheimer Feld 344, 69120 Heidelberg, Germany

³ German Center for Infection Research (DZIF), Heidelberg partner site, 69120 Heidelberg, Germany

⁴ Research School of Chemistry, Australian National University, Canberra, ACT 2601, Australia

ABSTRACT: Viral proteases have been established as drug targets in several viral diseases including human immunodeficiency virus and hepatitis C virus infections due to the essential role of these enzymes in virus replication. In contrast, no antiviral therapy is available to date against flaviviral infections including those by Zika virus (ZIKV), West Nile virus (WNV), or dengue virus (DENV). Numerous potent inhibitors of flaviviral proteases have been reported, however, a huge gap remains between the in-vitro and intracellular activities, possibly due to low cellular uptake of the charged compounds. Here, we present an alternative, nanoparticulate approach to antivirals. Conjugation of peptidomimetic inhibitors and cell-penetrating peptides to dextran yielded chemically defined nanoparticles that were potent inhibitors of flaviviral proteases. Peptide-dextran conjugates inhibited viral replication and infection in cells at non-toxic, low micromolar or even nanomolar concentrations. Thus, nanoparticulate antivirals might be alternative starting points for the development of broad-spectrum anti-flaviviral drugs.

Keywords. Flaviviral protease inhibitors, peptidomimetics, cell-penetrating, nanoparticulate inhibitors, multivalency

Flaviviruses are enveloped, single-stranded (+)-RNA viruses including the human pathogens yellow fever virus,¹ Japanese encephalitis virus,² tick-borne encephalitis virus³, dengue virus (DENV),⁴ West Nile virus (WNV), and Zika virus (ZIKV).⁵ Flaviviruses cause hundreds of millions of human infections every year leading to hundreds of thousands of severe cases and more than hundred thousand deaths.⁶ Only symptomatic therapies are available to date such as rehydration and treatment with paracetamol. Specific anti-flaviviral therapies have not been developed so far, although the medical need is high.⁵ There are vaccines against several of the flaviviruses, however, not against WNV and ZIKV, while the effectiveness of immunization against dengue virus is limited. Accordingly, the development of antivirals against several existing as well as newly emerging flaviviral species is of high medical relevance.

The development of broad-spectrum anti-flavivirals might be feasible due to the high conservation of some of the enzymes residing in the non-structural (NS) proteins.^{7, 8} Within the infected cell, seven flaviviral NS-proteins are produced,⁹ however, only the functions of the NS2B-NS3 and NS5 proteins have been studied in molecular detail.¹⁰ The NS5 protein bears the viral RNA-dependent RNA polymerase, the NS2B-NS3 complex has protease activity that is essential for the flaviviral replication cycle by cleaving the viral polyprotein into functional proteins. NS3 forms the catalytically active domain of the protease complex.¹¹ NS2B acts as co-factor for the protease-domain by supporting substrate binding and mediating membrane anchoring.^{12, 13} NS2B-NS3 is a serine protease with a trypsin-like fold, comprising the catalytic triad S135, H51 and D75.¹⁴ The enzyme recognizes oligobasic peptide sequences and cleaves between a P1 arginine or lysine residue and P1' amino acids with small side chains (glycine or serine).¹⁴⁻¹⁷

NS2B-NS3 is a promising drug target, since blocking proteases in other virus species, e.g. human immunodeficiency virus¹⁸ or hepatitis C virus,¹⁹ disrupts the replication cycle and has yielded

several clinically used antiviral drugs. Like for other proteases, peptides or peptidomimetics have been the main source of flaviviral inhibitors so far.^{20, 21} In many cases peptidomimetics with electrophilic head groups such as aldehydes and boronic acids, which are attacked by the nucleophilic serine residue of the catalytic triad, have been used as inhibitors of flavivirus proteases.^{13, 22-24} Binding specificity of peptides and peptidomimetics have been assured by the peptide sequences, which preferably contain the basic amino acids arginine and/or lysine in positions P1 and P2. P3 can be occupied either by another cationic side chain or by glycine, while P4 is preferably a hydrophobic amino acid residue.²⁵ Other peptidomimetics have been developed without the electrophilic center at the P1 residue. All oligobasic peptidomimetics are oligocations bearing several positive charges, which render many of them either inactive in cellular assays or reduce the cellular activity by several orders of magnitude relative to the biochemical assays, presumably due to the low cell penetration by compounds with a relative high charge density.²⁶⁻³⁴ In previous studies we demonstrated that peptide inhibitors cross membrane barriers efficiently on dextran nanocarriers containing few copies of a cell-penetrating peptide.³⁵ Beyond that, nanocarriers can improve the biocompatibility, solubility and stability against hydrolytic cleavage of peptide inhibitors.³⁶ Joshy et al. have shown the improved uptake of antiviral drugs using also a dextran nanocarrier.³⁷ Here we report a set of cell-penetrating, nanoparticulate inhibitors of the flaviviral NS2B-NS3 protease targeting both the membrane of the host cell for penetration and the substrate-binding pocket of several enzymes of this class. These novel, rationally designed inhibitors with validated binding modes might represent promising alternative starting points for the development of antivirals.

For the assembly of the nanoparticulate virus blockers inhibitory peptidomimetics were combined with transport peptides and fluorophores on a nanoparticulate carrier. As an inhibitory com-

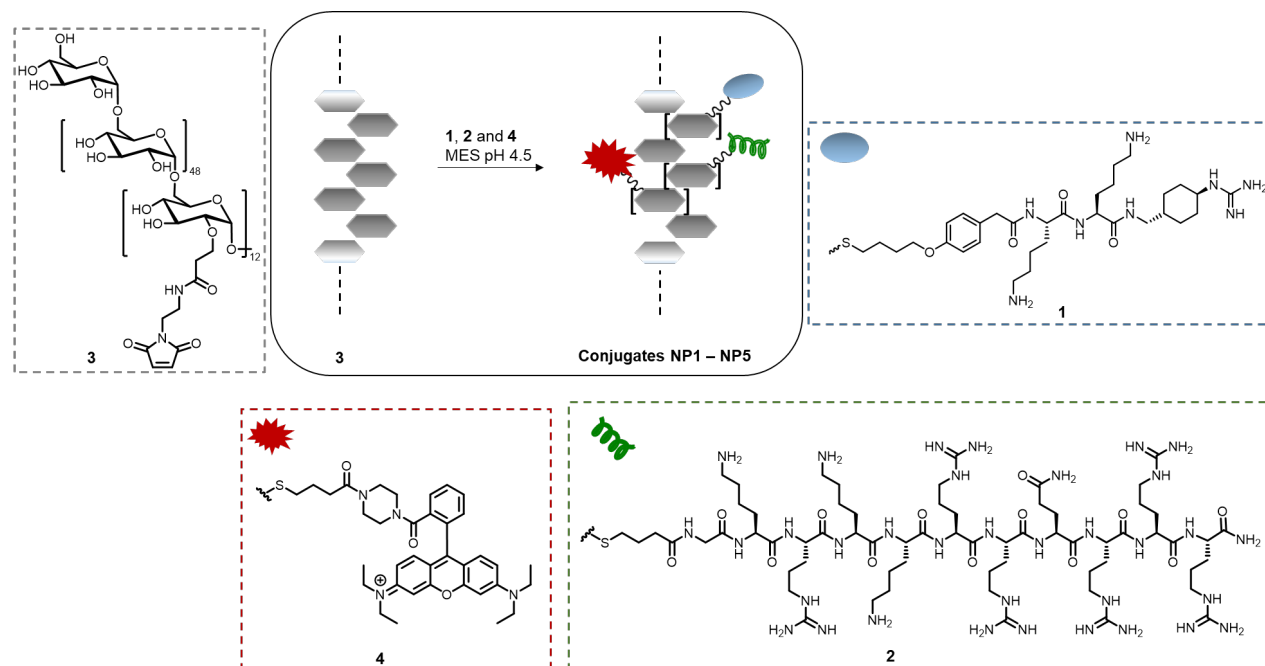
ponent, the thiol-modified peptidomimetic **1** was designed carrying a decarboxylated arginine-mimicking fragment at the C-terminal P1 position, two lysins in P2 and P3, and a 4-(4-mercapto-butoxy)-phenyl-acetyl residue for conjugation in P4. (Scheme 1). **1** fitted well into the active site of WNV^{Pro} (see Figure S13). It is a derivative of potent inhibitors of the NS2B-NS3 protein of WNV published recently by Steinmetzer et al.³⁸ The best compound of the Steinmetzer series had the 3,4-dichloro-phenylacetyl group in P4 and displayed a K_i value of 120 nM in the enzymatic assay, however, in infected cells no antiviral effect was reported, presumably due to insufficient cell permeability of these oligocationic peptidomimetics.³⁹

Recently, we have established that polymeric nanoparticles carrying bioactive molecules, can penetrate cell membranes by conjugation with cell penetrating peptides.^{35,40} Coupling of peptides to carrier polymers led to the strong amplification of biological activity in cells and a higher proteolytic stability. Thus, to enable the entry of the nanoparticulate inhibitors into the cell, we employed the cell-penetrating TAT dodeca-peptide **2** (GRKKRRQRRRPK).⁴¹ This peptide was modified with an N-terminal thiol-label to enable conjugation to the nanoparticle (Scheme 1). Several polymer backbones have been investigated and linear dextran was found to be superior to polymeric *N*-(2-hydroxypropyl)-methacrylamide (pHPMG) and hyper-dendritic poly-glycerol (hPG) in generating high-affinity nanoparticles.⁴⁰ For coupling of several different thiol-labeled peptides, peptidomimetics and fluorophores to the dextran backbone in one step, conjugation to 2-maleimido-dextran **3** was found to be advantageous to other strategies. For microscopic tracking of the nanoparticles, the *N,N,N',N'*-tetra-ethyl-rhodamine **4** was prepared as a thiol-labeled fluorophore for the microscopic tracking of the obtained nanoparticles (SI 1.5.1, Figure S18). The protected C-terminal fragment of peptidomimetic **1**, *trans-N,N'*-di-Boc-(4-amino-methyl)-cyclohexanyl-guanidine **6**, was

synthesized in four steps from *trans*-(*N*-Boc-4-aminomethyl)-cyclohexyl-amine **5** (Scheme 2a). To enable the modification at the N-terminus of the peptidomimetic, compound **8** was synthesized carrying an *S*-trityl-protected thiol for use in peptide synthesis and for later coupling of the peptidomimetic to the dextran carrier (Scheme 2b). For assembly of the peptidomimetic inhibitor **1**, *N*-Fmoc-Lys(Boc) was coupled to 2-chloro-trityl resin in DCM using DIPEA as a base. After *N*-Fmoc-deprotection with piperidine-DMF, a second lysine residue was condensed to the amino group followed by *N*-Fmoc cleavage. Acid **8** was coupled to the unprotected N-terminus of the dipeptide and the protected product **9** was released from the resin employing hexafluoro-isopropanol. Compound **9** was activated in solution and coupled to the Boc-protected building block **6** (Scheme 2c). After deprotection, the peptidomimetic **1** was obtained.

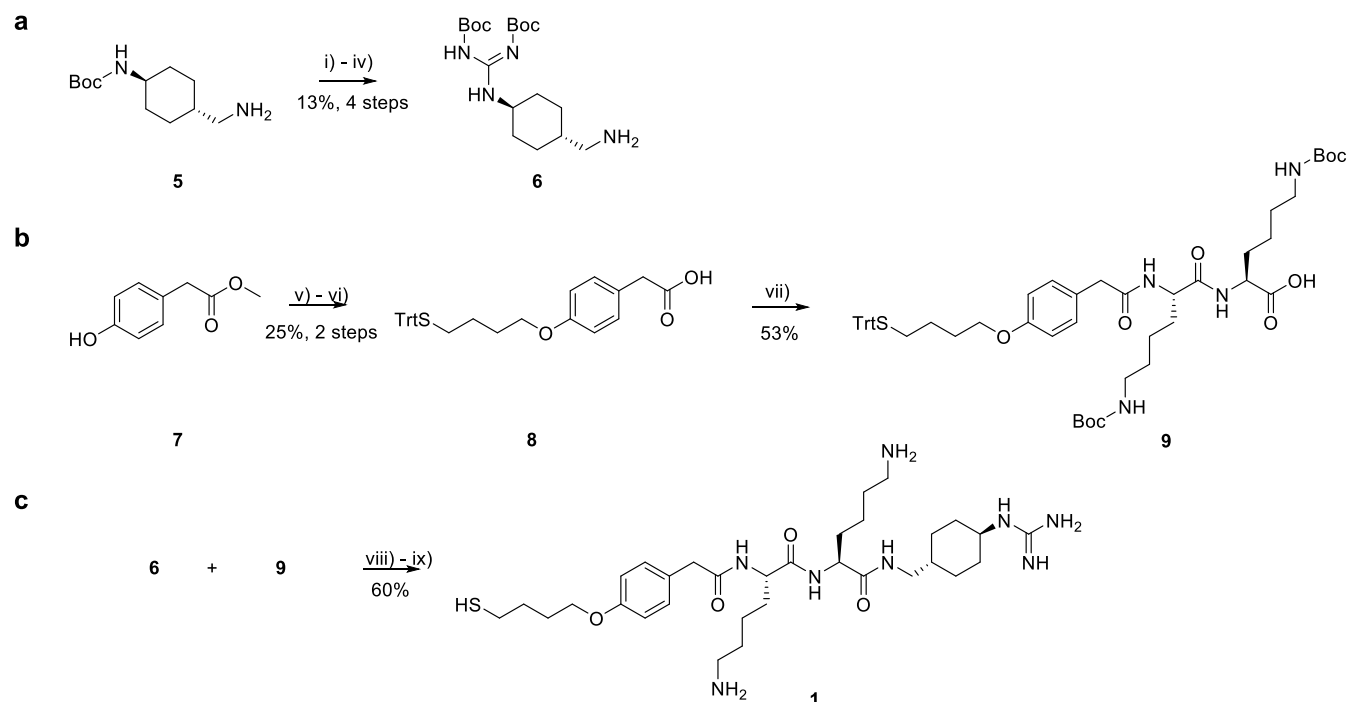
Subsequently, peptidomimetic inhibitor **1**, TAT-peptide **2** and the rhodamine fluorophore **4** were conjugated to 2-maleimido-dextran **3** to furnish loaded nanoparticles NP1-NP5 (Table 1). All conjugation reactions were performed in 10 mM MOPS buffer at pH 4.5 granting the full protonation of basic lysine and arginine residues and selective reactivity of the nucleophilic thiol residues with maleimides. NP1 loaded with 2.6 copies of TAT-peptide **2** and 0.5 copies of the fluorophore was obtained by conjugation of **3** with 3 equiv. of peptide **2** and 4.5 equiv. of fluorophore **4** (SI 1.2.7). NP2 and NP3 with 2.0 and 4.0 copies of inhibitor **1** attached were generated from NP1 by conjugation with 8.4 and 16.3 equiv. of free inhibitor **1**, respectively (SI 1.2.8). NP4 and NP5 carrying 3.6 and 6.0 copies of inhibitor **1** were synthesized through the conjugation of carrier **3** with 8.9 and 17.8 equiv of **1**, respectively, together with 11.3 and 10.9 equiv of fluorophore **4** (0.5 copies) (SI 1.2.9). Loadings of all nanoparticles were determined by a combination of ¹H-NMR and UV-Vis spectroscopy (SI 1.3).

Scheme 1. General strategy for the construction of nanoparticulate virus blockers



Flaviviral inhibitor **1**, the cell-penetrating TAT-peptide **2**, and rhodamine fluorophore **4** were synthesized carrying terminal 4-mercapto-butoxy or 4-mercapto-butyrylamido residues. These thiol labels enabled the simultaneous conjugation of compound **1**, **2** and **4** to 2-maleimido-dextran **3**.

Scheme 2. Synthesis of peptidomimetic **1**



Reaction conditions: **i**) Cbz-Cl, DIPEA, THF, rt, 16 h. **ii**) TFA/DCM, 0°C, 2h. **iii**) 1,3-di-Boc-2-(trifluoromethylsulfonyl)-guanidine, NEt₃, DCM, rt, 16 h. **iv**) Pd/C, H₂, MeOH, rt, 2 h. **v**) 1,4-diiodobutane, K₂CO₃, acetone, 50 °C, 16 h. **vi**) triphenylmethanethiol, THF, KOtBu, 70 °C, 1 h; 1 M NaOH, THF, 70 °C, 2 h. **vii**) SPPS with 2-Cl-Trt-resin, Fmoc-Lys(Boc)-OH, DCM, DIPEA, 16 h, rt. **viii**) DCM, EDC, HOBt, **10**, rt, 16 h; **ix**) 82.5% TFA/ 5% phenol/ 5% H₂O/ 5% thioanisole/ 2.5% EDT, rt, 2 h.

The peptidomimetics, peptides and conjugates were tested in enzymatic assays with WNV^{Pro}, ZIKV^{Pro}, and DENV^{Pro} using the fluorogenic substrate Boc-GKR-AMC for WNV^{Pro} and ZIKV^{Pro}, and Boc-GRR-AMC for DENV^{Pro}. All measurements were performed at pH 8.5 in 50 mM Tris-HCl with 20% (v/v) glycerol (SI 1.4.2). Peptidomimetic **1** displayed *K_I* values of 343 nM for WNV^{Pro} and 79 nM for ZIKV^{Pro}, respectively, in good agreement with data published for similar compounds without the thiol-linker (**Table 1**).³⁸ Inhibition of DENV^{Pro} was weaker, an effect reported before for similar peptidomimetics.³⁹ TAT peptide **2** also showed strong inhibition with a *K_I* of 96 nM for WNV^{Pro} and a *K_I* of 140 nM for ZIKV^{Pro}. Presumably, the NS2B-NS3 protease binds to the nine basic lysine or arginine residues of the TAT sequence fitting well to reported inhibitor sequences.⁴²

Next, inhibitory activities of the conjugated nanoparticles were determined. **NP4** loaded with 3.6 copies of inhibitor **1** but no TAT peptide displayed a *K_I* of 304 nM (WNV^{Pro}), similar to the free inhibitor **1**. Loading of **NP5** with 6 copies led to an improved *K_I* of 103 nM. The increased local concentration and multivalent presentation of the inhibitor **1** in the nanoparticle **NP5** might contribute to the amplified inhibition by **NP5**.⁴³ In contrast, **NP1**, carrying 2.6 copies of TAT peptide **2** showed a *K_I* of 150 nM (WNV^{Pro}), making it a less potent inhibitor than free TAT-peptide **2**. Strongly enhanced inhibition, however, was observed for hetero-multivalent constructs **NP2** and **NP3** containing both peptidomimetic **1** and TAT-peptide **2**. Combination of 2 copies of **1** with 2.6 copies of **2** in **NP2** boosted the *K_I* values to 33 nM for WNV^{Pro} and 51 nM for ZIKV^{Pro}. The effect was even stronger for **NP3** with 4 copies of **1** and 2.6

copies of **2** resulting in remarkable *K_I* values of 9 nM for WNV^{Pro} and 34 nM for ZIKV^{Pro}. For control, unloaded dextran was tested and did not show any inhibitory activity (**Figure S14**). Since **NP1**, **NP4**, and **NP5** with only TAT-peptide **2** or only inhibitor **1** were much weaker inhibitors than **NP2** and **NP3**, it can be concluded that the hetero-multivalent presentation of peptidomimetic **1** with TAT **2** led to this remarkable improvement of the *IC₅₀* values.

Subsequently, we investigated the cellular activity of the hetero-multivalent conjugates **NP2**, **3**, and **5**. Efficient cellular uptake was detected for **NP2** and **3** at low μM concentrations by fluorescence microscopy (**Figure S18**). This suggested that these conjugates might be effective inhibitors of viral replication in flavivirus-infected human cells. In order to determine concentrations tolerated by Huh7 cells, nanoparticles were tested in a CellTiterGlo® assay measuring intracellular ATP levels (SI 1.5.2., **Figure S19**). While **NP5** (without TAT peptide **2**) did not affect cell viability even at concentrations higher than 25 μM **NP2** and **NP3** (both with TAT peptide **2**) reduced cellular ATP levels at 25 μM. This might be due to the low cell permeability of **NP5** since it is not carrying the cell penetrating peptide **2**. As there was no effect of all three tested nanoparticles on cell viability at a concentration of 12.5 μM, antiviral effects of the conjugates were investigated at or below this concentration. Antiviral activities of inhibitors **NP2**, **NP3**, and **NP5** against WNV and DENV were determined by measuring the amount of infectious virus progeny released from compound-treated cells (**Figure 1a-c**, **Table 2** and **Figure S20**). In these assays, the inhibitor was added to virus-infected Huh7 cells and culture supernatants were harvested 48 h later.

Table 1. Inhibition of WNV^{Pro}, ZIKV^{Pro}, and DENV^{Pro} by nanoparticles NP1-NP5. For raw data and S.D. see SI; K_I -values have been determined using the Cheng-Prusoff equation.

		1	2	NP1	NP2	NP3	NP4	NP5
Nano-particle loading with	1				2.0	4.0	3.6	6.0
	2			2.6	2.6	2.6		
	4			0.5	0.5	0.5	0.5	0.5
IC_{50} [nM]	WNV ^{Pro}	460	129	201	45	12	408	139
	ZIKV ^{Pro}	125	223	n.d.	82	54	n.d.	n.d.
	DENV ^{Pro}	17070	11140	n.d.	921	4619	n.d.	n.d.
K_I [nM]	WNV ^{Pro}	343	96	150	33	9	304	103
	ZIKV ^{Pro}	79	140	n.d.	51	34	n.d.	n.d.
	DENV ^{Pro}	12739	8313	n.d.	687	3447	n.d.	n.d.

The amount of infectious virus contained therein was determined by plaque assays. Ribavirin was used as positive control. Inhibition of the virus replication was determined in relation to the negative control. In WNV-infected cells **NP2** and **NP3** inhibited virus replication effectively. At a concentration of 12.5 μ M **NP2** reduced WNV titers by about 67% while **NP3** showed an inhibition by 78%. At a concentration of 6.25 μ M, the conjugate **NP3** still displayed an inhibition of 54%, indicating an estimated EC_{50} value of **NP3** around 6.25 μ M. For DENV significantly higher antiviral activities of the conjugates were observed (**Figure 1b**). Virus titers were reduced by 98% and more when infected cells were cultured in presence of 6.25 to 12.5 μ M **NP2** or **NP3**. In contrast, in presence of 6.25 to 25 μ M **NP5** a remaining activity of 5-10% was detected, indicating the importance of TAT-coupling for inhibition. As Ribavirin reduced virus replication only about 25% at a concentration of 12.5 μ M, the synthesized conjugates **NP2** and **NP3** showed a much better inhibition of DENV replication. Thus, inhibition of plaque formation was measured at even lower concentrations of nanoparticles (**Figure 1c**). The hetero-multivalent conjugates **NP2** and **NP3** inhibited viral replication between 90-98% at 2.5 μ M while **NP5** without the cell-penetrating TAT peptide **2** showed almost no inhibition at this concentration. **NP2** with 2 copies of **1** reduced viral replication around 40% at a concentration of 0.25 μ M, while **NP3** with 4 copies of **1** reduced viral replication by around 75% at a concentration of 0.1 μ M suggesting a remarkable nanomolar EC_{50} value of <0.1 μ M.

To determine the activity of the conjugates on ZIKV replication, Huh7 cells were infected with a luciferase reporter virus

derived from the MR766 strain.⁴⁴ Antiviral activity was determined by measuring luciferase activity in infected cells reflecting RNA replication (**Figure 1d**). The hetero-multivalent conjugates **NP2** and **NP3** inhibited ZIKV replication at a concentration of 12.5 μ M by 71 and 72%, respectively (EC_{50} < 12.5 μ M). The nanoparticle **NP5** (without TAT **2**) did not show inhibition at this concentration, but required a concentration of 25 μ M to reach 40% inhibition. As a result, also for ZIKV the incorporation of TAT **2** into the conjugate was crucial to enter the host cells and inhibit the replication of the virus.

Here we demonstrated design, synthesis, and biochemical evaluation of nanoparticular virus blockers. A peptidomimetic showing inhibition of WNV^{Pro} *in-vitro* but no antiviral effect in cells was coupled to a dextran backbone. In addition, cell penetrating TAT peptide was conjugated to the polymer. The obtained nanoparticular conjugates were low nanomolar inhibitors of WNV^{Pro} and ZIKV^{Pro} and less active for DENV^{Pro}. Incorporation of several copies of the inhibitor resulted in a strong increase of inhibition both in the enzyme assay and in cells. Cell penetrating TAT peptide also inhibited viral proteases and incorporation of TAT into the conjugates strongly enhanced cellular uptake and boosted antiviral activities against WNV, DENV and ZIKV in the cell-based assays, most pronounced for DENV. In perspective, nanoparticular virus blockers might overcome limitations of peptidomimetic inhibitors due to enhanced cell permeability and cellular activity and future experiments will reveal details of their mode of action.

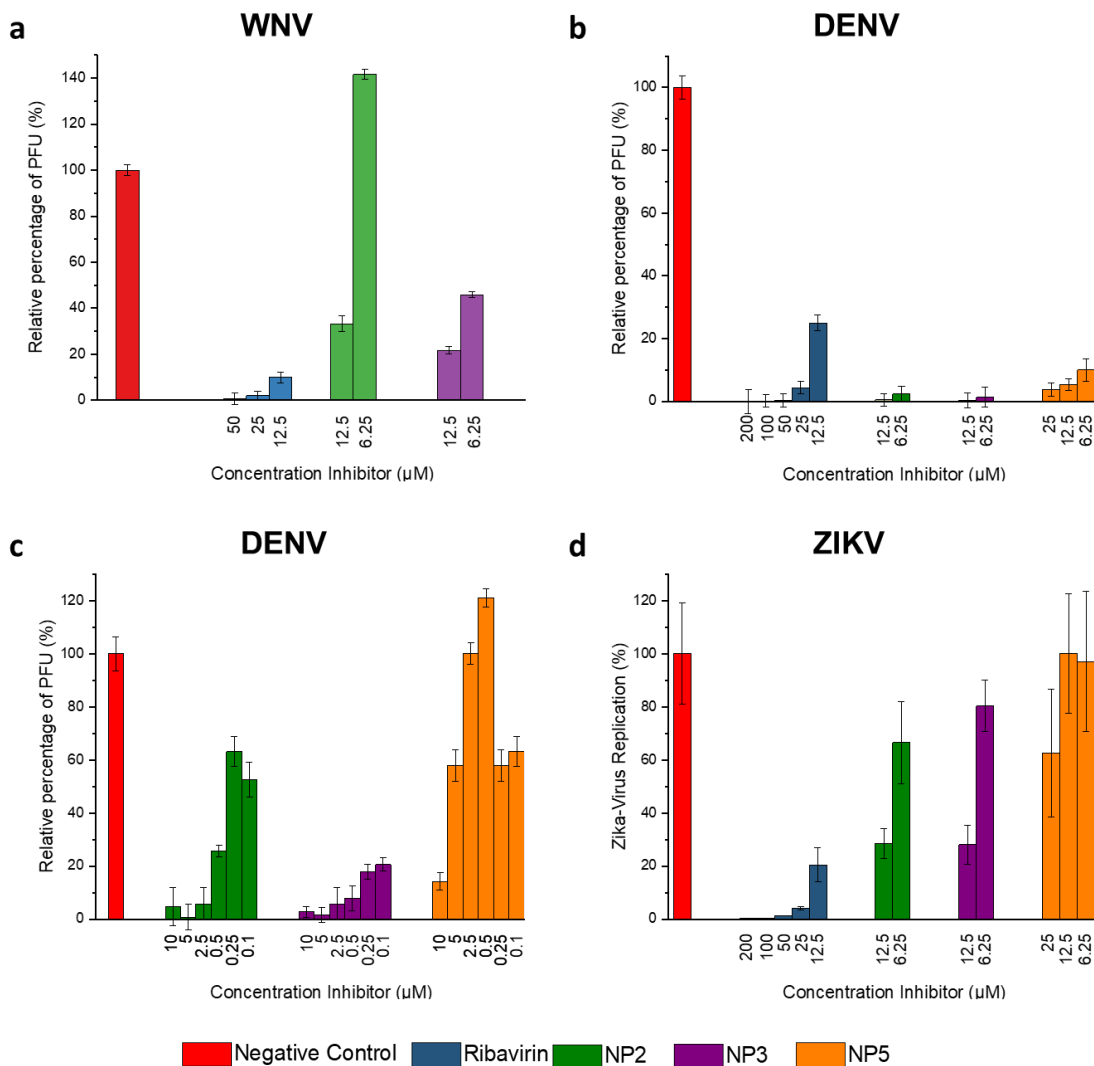


Figure 1. Inhibition of virus replication in infected Huh7 cells. For WNV (a) and DENV (b,c) virus inhibition was determined in the plaque assay measuring the amount of infectious virus released into the culture supernatant of infected cells (see **Figure S20** for graphs in log PFU/ml). For ZIKV (d) a Renilla luciferase reporter virus of the MR766 strain was used and inhibition of virus replication was measured in infected cells by quantifying luciferase activity reflecting viral RNA replication. In all experiments the multiplicity of infection (MOI) was 0.1. 48 h after infection, culture supernatants were harvested for plaque assay (in case of WNV and DENV) and cell lysates for luciferase assay (in case of ZIKV). Ribavirin served as positive control (blue bars). Values obtained with solvent-treated infected cells (red bars) were set to 100% and used to normalize values obtained with inhibitor-treated infected cells. Estimated EC_{50} values of NP3 are ~6.25 μ M for WNV, <0.1 μ M for DENV, and <12.5 μ M for ZIKV.

Table 2. Inhibition of WNV, ZIKV and DENV replication in infected cells.

		NP2			NP3			NP5			Ribavirin
		12.5 μ M	6.25 μ M	0.1 μ M	12.5 μ M	6.25 μ M	0.1 μ M	12.5 μ M	6.25 μ M	0.1 μ M	12.5 μ M
Nano-particle loading with	1	2.0			4.0			6.0			
	2	2.6			2.6						
	4	0.5			0.5			0.5			
Inhibition of Viral Replication [%]	WNV	67	0	n.d.	78	54	n.d.	n.d.	n.d.	n.d.	90
	DENV	100	98	47	100	99	79	95	90	37	75
	ZIKV	71	34	n.d.	72	20	n.d.	0	0	n.d.	80

ASSOCIATED CONTENT

Supporting Information (SI)

This material is available free of charge via the Internet at <http://pubs.acs.org>.

AUTHOR INFORMATION

Corresponding Author

* E-mail: joerg.rademann@fu-berlin.de

ACKNOWLEDGEMENT

The authors thank Prof. Tanja Schirmeister, Mainz, and Prof. Rolf Hilgenfeld, Lübeck, for providing us with the vectors of DENV and WNV protease. J.R. thanks the Deutsche Forschungsgemeinschaft (DFG) for funding (SFB 765, SFB 1349, Ra895-11) and the Australian National University for a visiting fellowship. E.M. thanks the DAAD for a fellowship. C.N. thanks the Australian Research Council for a Discovery Early Career Research Award (DE190100015) and the Freie Universität Berlin for a Rising Star fellowship.

ABBREVIATIONS

NP – nanoparticulate virus blockers

ZIKV – Zika Virus

ZIKV^{Pro} – Zika Virus Protease

WNV – West Nile Virus

WNV^{Pro} – West Nile Virus Protease

DENV – Dengue Virus

DENV^{Pro} – Dengue Virus Protease

NS – non-structural

CPP – cell penetrating peptide

REFERENCES

1. Theiler, M.; Smith, H. H., The Use of Yellow Fever Virus Modified by in Vitro Cultivation for Human Immunization. *J. Exp. Med.* **1937**, *65*, 787-800.
2. Srivastava, A. K.; Putnak, J. R.; Lee, S. H.; Hong, S. P.; Moon, S. B.; Barvir, D. A.; Zhao, B.; Olson, R. A.; Kim, S.-O.; Yoo, W.-D.; Towle, A. C.; Vaughn, D. W.; Innis, B. L.; Eckels, K. H., A purified inactivated Japanese encephalitis virus vaccine made in vero cells. *Vaccine* **2001**, *19*, 4557-4565.
3. Zent, O.; Banzhoff, A.; Hilbert, A. K.; Meriste, S.; Szuzewski, W.; Wittermann, C., Safety, immunogenicity and tolerability of a new pediatric tick-borne encephalitis (TBE) vaccine, free of protein-derived stabilizer. *Vaccine* **2003**, *21*, 3584-3592.
4. Guy, B.; Barrere, B.; Malinowski, C.; Saville, M.; Teysou, R.; Lang, J., From research to phase III: preclinical, industrial and clinical development of the Sanofi Pasteur tetravalent dengue vaccine. *Vaccine* **2011**, *29*, 7229-7241.
5. Chesnut, M.; Munoz, L. S.; Harris, G.; Freeman, D.; Gama, L.; Pardo, C. A.; Pamies, D., In vitro and in silico Models to Study Mosquito-Borne Flavivirus Neuropathogenesis, Prevention, and Treatment. *Front. Cell. Infect. Microbiol.* **2019**, *9*, 223.
6. Guzman, M. G.; Harris, E., Dengue. *Lancet* **2015**, *385*, 453-465.
7. Boldescu, V.; Behnam, M. A. M.; Vasilakis, N.; Klein, C. D., Broad-spectrum agents for flaviviral infections: dengue, Zika and beyond. *Nat. Rev. Drug Discov.* **2017**, *16*, 565-586.
8. Pach, S.; Sarter, T. M.; Yousef, R.; Schaller, D.; Bergemann, S.; Arkona, C.; Rademann, J.; Nitsche, C.; Wolber, G., Catching a Moving Target: Comparative Modeling of Flaviviral NS2B-NS3 Reveals Small Molecule Zika Protease Inhibitors. *ACS Med. Chem. Lett.* **2020**, *11*, 514-520.
9. Simmonds, P.; Becher, P.; Bukh, J.; Gould, E. A.; Meyers, G.; Monath, T.; Muerhoff, S.; Pletnev, A.; Rico-Hesse, R.; Smith, D. B.; Stapleton, J. T.; Ictv Report, C., ICTV Virus Taxonomy Profile: Flaviviridae. *J. Gen. Virol.* **2017**, *98*, 2-3.
10. Barrows, N. J.; Campos, R. K.; Liao, K. C.; Prasanth, K. R.; Soto-Acosta, R.; Yeh, S. C.; Schott-Lerner, G.; Pompon, J.; Sessions, O. M.; Bradrick, S. S.; Garcia-Blanco, M. A., Biochemistry and Molecular Biology of Flaviviruses. *Chem. Rev.* **2018**, *118*, 4448-4482.
11. Assenberg, R.; Mastrangelo, E.; Walter, T. S.; Verma, A.; Milani, M.; Owens, R. J.; Stuart, D. I.; Grimes, J. M.; Mancini, E. J., Crystal structure of a novel conformational state of the flavivirus NS3 protein: implications for polyprotein processing and viral replication. *J. Virol.* **2009**, *83*, 12895-12906.
12. Falgout, B.; Pethel, M.; Zhang, Y. M.; Lai, C. J., Both nonstructural proteins NS2B and NS3 are required for the proteolytic processing of dengue virus nonstructural proteins. *J. Virol.* **1991**, *65*, 2467-2475.
13. Erbel, P.; Schiering, N.; D'Arcy, A.; Renatus, M.; Kroemer, M.; Lim, S. P.; Yin, Z.; Keller, T. H.; Vasudevan, S. G.; Hommel, U., Structural basis for the activation of flavivirus NS3 proteases from dengue and West Nile virus. *Nat. Struct. Mol. Biol.* **2006**, *13*, 372-373.
14. Bazan, J. F.; Fletterick, R. J., Detection of a trypsin-like serine protease domain in flaviviruses and pestviruses. *Virol. J.* **1989**, *171*, 637-639.
15. Nall, T. A.; Chappell, K. J.; Stoermer, M. J.; Fang, N. X.; Tyndall, J. D.; Young, P. R.; Fairlie, D. P., Enzymatic characterization and homology model of a catalytically active recombinant West Nile virus NS3 protease. *J. Biol. Chem.* **2004**, *279*, 48535-48542.
16. Chappell, K. J.; Nall, T. A.; Stoermer, M. J.; Fang, N. X.; Tyndall, J. D.; Fairlie, D. P.; Young, P. R., Site-directed mutagenesis and kinetic studies of the West Nile Virus NS3 protease identify key enzyme-substrate interactions. *J. Biol. Chem.* **2005**, *280*, 2896-2903.
17. Li, J.; Lim, S. P.; Beer, D.; Patel, V.; Wen, D.; Tumanut, C.; Tully, D. C.; Williams, J. A.; Jiricek, J.; Priestle, J. P.; Harris, J. L.; Vasudevan, S. G., Functional profiling of recombinant NS3 proteases from all four serotypes of dengue virus using tetrapeptide and octapeptide substrate libraries. *J. Biol. Chem.* **2005**, *280*, 28766-28774.
18. Ghosh, A. K.; Osswald, H. L.; Prato, G., Recent Progress in the Development of HIV-1 Protease Inhibitors for the Treatment of HIV/AIDS. *J. Med. Chem.* **2016**, *59*, 5172-5208.
19. Asselah, T.; Boyer, N.; Saadoun, D.; Martinot-Peignoux, M.; Marcellin, P., Direct-acting antivirals for the treatment of hepatitis C virus infection: optimizing current IFN-free treatment and future perspectives. *Liver Int.* **2016**, *36*, 47-57.
20. Lima, A. B.; Behnam, M. A. M.; Sherif, Y. E.; Nitsche, C.; Vecchi, S. M.; Klein, C. D., Dual inhibitors of the dengue and West Nile virus NS2B-NS3 proteases: Synthesis, biological evaluation and docking studies of novel peptide-hybrids. *Bioorg. Med. Chem.* **2015**, *23*, 5748-5755.
21. da Silva-Júnior, E. F.; de Araújo-Júnior, J. X., Peptide derivatives as inhibitors of NS2B-NS3 protease from Dengue, West Nile, and Zika flaviviruses. *Bioorg. Med. Chem.* **2019**, *27*, 3963-3978.

22. Lei, J.; Hansen, G.; Nitsche, C.; Klein, C. D.; Zhang, L.; Hilgenfeld, R., Crystal structure of Zika virus NS2B-NS3 protease in complex with a boronate inhibitor. *Science* **2016**, *353*, 503-505.
23. Nitsche, C.; Steuer, C.; Klein, C. D., Arylcyanocrylamides as inhibitors of the Dengue and West Nile virus proteases. *Bioorg. Med. Chem.* **2011**, *19*, 7318-7337.
24. Yin, Z.; Patel, S. J.; Wang, W. L.; Wang, G.; Chan, W. L.; Ranga Rao, K. R.; Alam, J.; Jeyaraj, D. A.; Ngeq, X.; Patel, V.; Beer, D.; Pheng Lim, S.; Vasudevan, S. G.; Keller, T. H., Peptide inhibitors of Dengue virus NS3 protease. Part 1: Warhead. *Bioorg. Med. Chem.* **2006**, *16*, 36-39.
25. Rut, W.; Zhang, L.; Kasperkiewicz, P.; Poreba, M.; Hilgenfeld, R.; Drag, M., Extended substrate specificity and first potent irreversible inhibitor/activity-based probe design for Zika virus NS2B-NS3 protease. *Antivir. Res.* **2017**, *139*, 88-94.
26. Li, Y.; Zhang, Z.; Phoo, W. W.; Loh, Y. R.; Li, R.; Yang, H. Y.; Jansson, A. E.; Hill, J.; Keller, T. H.; Nacro, K.; Luo, D.; Kang, C., Structural Insights into the Inhibition of Zika Virus NS2B-NS3 Protease by a Small-Molecule Inhibitor. *Structure* **2018**, *26*, 555-564 e3.
27. Lee, H.; Ren, J.; Nocadello, S.; Rice, A. J.; Ojeda, I.; Light, S.; Minasov, G.; Vargas, J.; Nagarathnam, D.; Anderson, W. F.; Johnson, M. E., Identification of novel small molecule inhibitors against NS2B/NS3 serine protease from Zika virus. *Antivir. Res.* **2017**, *139*, 49-58.
28. Yao, Y.; Huo, T.; Lin, Y. L.; Nie, S.; Wu, F.; Hua, Y.; Wu, J.; Kneubehl, A. R.; Vogt, M. B.; Rico-Hesse, R.; Song, Y., Discovery, X-ray Crystallography and Antiviral Activity of Allosteric Inhibitors of Flavivirus NS2B-NS3 Protease. *J. Am. Chem. Soc.* **2019**, *141*, 6832-6836.
29. Rassias, G.; Zogali, V.; Swarbrick, C. M. D.; Ki Chan, K. W.; Chan, S. A.; Gwee, C. P.; Wang, S.; Kaplanai, E.; Canko, A.; Kioussis, D.; Lescar, J.; Luo, D.; Matsoukas, M. T.; Vasudevan, S. G., Cell-active carbazole derivatives as inhibitors of the Zika virus protease. *Eur. J. Med. Chem.* **2019**, *180*, 536-545.
30. Millies, B.; von Hammerstein, F.; Gellert, A.; Hammerschmidt, S.; Barthels, F.; Goppel, U.; Immerheiser, M.; Elgner, F.; Jung, N.; Basic, M.; Kersten, C.; Kiefer, W.; Bodem, J.; Hildt, E.; Windbergs, M.; Hellmich, U. A.; Schirmeister, T., Proline-based allosteric inhibitors of Zika and Dengue virus NS2B/NS3 proteases. *J. Med. Chem.* **2019**, *62*, 11359-11382.
31. Brecher, M.; Li, Z.; Liu, B.; Zhang, J.; Koetzner, C. A.; Alifarag, A.; Jones, S. A.; Lin, Q.; Kramer, L. D.; Li, H., A conformational switch high-throughput screening assay and allosteric inhibition of the flavivirus NS2B-NS3 protease. *PLoS Pathog.* **2017**, *13*, e1006411.
32. Shiryaev, S. A.; Farhy, C.; Pinto, A.; Huang, C. T.; Simonetti, N.; Elong Ngono, A.; Dewing, A.; Shresta, S.; Pinkerton, A. B.; Cieplak, P.; Strongin, A. Y.; Terskikh, A. V., Characterization of the Zika virus two-component NS2B-NS3 protease and structure-assisted identification of allosteric small-molecule antagonists. *Antiviral. Res.* **2017**, *143*, 218-229.
33. Roy, A.; Lim, L.; Srivastava, S.; Lu, Y.; Song, J., Solution conformations of Zika NS2B-NS3pro and its inhibition by natural products from edible plants. *PLoS ONE* **2017**, *12*, e0180632.
34. Yuan, S.; Chan, J. F.; den-Haan, H.; Chik, K. K.; Zhang, A. J.; Chan, C. C.; Poon, V. K.; Yip, C. C.; Mak, W. W.; Zhu, Z.; Zou, Z.; Tee, K. M.; Cai, J. P.; Chan, K. H.; de la Pena, J.; Perez-Sanchez, H.; Ceron-Carrasco, J. P.; Yuen, K. Y., Structure-based discovery of clinically approved drugs as Zika virus NS2B-NS3 protease inhibitors that potently inhibit Zika virus infection in vitro and in vivo. *Antivir. Res.* **2017**, *145*, 33-43.
35. Richter, M.; Chakrabarti, A.; Ruttekolk, I. R.; Wiesner, B.; Beyermann, M.; Brock, R.; Rademann, J., Multivalent design of apoptosis-inducing bid-BH3 peptide-oligosaccharides boosts the intracellular activity at identical overall peptide concentrations. *Chem. Eur. J.* **2012**, *18*, 16708-16715.
36. Ruttekolk, I. R.; Chakrabarti, A.; Richter, M.; Verdurmen, W. P. R.; Duchardt, F.; Glauner, H.; Rademann, J.; Brock, R., Coupling to polymeric scaffolds stabilizes biofunctional peptides for intracellular applications. *Mol. Pharmacol.* **2011**, *79*, 692-700.
37. Joshy, K. S.; Anne, G.; Snigdy, S.; Blessy, J.; Nandykumar, K.; Laly, P. A.; Sabu, T., Novel core-shell dextran hybrid nanosystem for anti-viral drug delivery. *Mater. Sci. Eng. A* **2018**, *93*, 864-872.
38. Hammamy, M. Z.; Haase, C.; Hammami, M.; Hilgenfeld, R.; Steinmetzer, T., Development and Characterization of New Peptidomimetic Inhibitors of the West Nile Virus NS2B-NS3 Protease. *ChemMedChem* **2013**, *8*, 231-241.
39. Kouretova, J.; Hammamy, M. Z.; Epp, A.; Harges, K.; Kallis, S.; Zhang, L. L.; Hilgenfeld, R.; Bartenschlager, R.; Steinmetzer, T., Effects of NS2B-NS3 protease and furin inhibition on West Nile and Dengue virus replication. *J. Enzym Inhib. Med. Chem.* **2017**, *32*, 712-721.
40. Koschek, K.; Durmaz, V.; Krylova, O.; Wiczorek, M.; Gupta, S.; Richter, M.; Bujotzek, A.; Fischer, C.; Haag, R.; Freund, C.; Weber, M.; Rademann, J., Peptide-polymer ligands for a tandem WW-domain, an adaptive multivalent protein-protein interaction: lessons on the thermodynamic fitness of flexible ligands. *Beilstein J. Org. Chem.* **2015**, *11*, 837-847.
41. Richard, J. P.; Melikov, K.; Vives, E.; Ramos, C.; Verbeure, B.; Gait, M. J.; Chernomordik, L. V.; Lebleu, B., Cell-penetrating Peptides - A Reevaluation of the Mechanism of cellular uptake. *J. Biol. Chem.* **2003**, *278*, 585-590.
42. Shiryaev, S. A.; Ratnikov, B. I.; Chekanov, A. V.; Sikora, S.; Rozanov, D. V.; Godzik, A.; Wang, J.; Smith, J. W.; Huang, Z.; Lindberg, I.; Samuel, M. A.; Diamond, M. S.; Strongin, A. Y., Cleavage targets and the D-arginine-based inhibitors of the West Nile virus NS3 processing proteinase. *Biochem. J.* **2006**, *393*, 503-511.
43. Fasting, C.; Schalley, C. A.; Weber, M.; Seitz, O.; Hecht, S.; Koksche, B.; Dervede, J.; Graf, C.; Knapp, E.-W.; Haag, R., Multivalency as a Chemical Organization and Action Principle. *Angew. Chem. Int. Ed.* **2012**, *51*, 2-29.
44. Münster, M.; Płaszczycza, A.; Cortese, M.; Neufeldt, C. J.; Goellner, S.; Long, G.; Bartenschlager, R., A Reverse Genetics System for Zika Virus Based on a Simple Molecular Cloning Strategy. *Viruses* **2018**, *10*, 368.